AIP Journal of Applied Physics

Exploring the alignment of carbon nanotubes dispersed in a liquid crystal matrix using coplanar electrodes

D. Volpati, M. K. Massey, D. W. Johnson, A. Kotsialos, F. Qaiser, C. Pearson, K. S. Coleman, G. Tiburzi, D. A. Zeze, and M. C. Petty

Citation: Journal of Applied Physics **117**, 125303 (2015); doi: 10.1063/1.4916080
View online: http://dx.doi.org/10.1063/1.4916080
View Table of Contents: http://scitation.aip.org/content/aip/journal/jap/117/12?ver=pdfcov
Published by the AIP Publishing

Exploring the alignment of carbon nanotubes dispersed in a liquid crystal matrix using coplanar electrodes

D. Volpati,[1,2] M. K. Massey,[1] D. W. Johnson,[3] A. Kotsialos,[1] F. Qaiser,[1] C. Pearson,[1] K. S. Coleman,[3] G. Tiburzi,[1] D. A. Zeze,[1] and M. C. Petty[1]
[1]*School of Engineering and Computing Sciences and Centre for Molecular and Nanoscale Electronics, Durham University, South Road, Durham DH1 3LE, United Kingdom*
[2]*São Carlos Institute of Physics, São Paulo University–USP, PO Box 369, 13566-590, São Carlos, SP, Brazil*
[3]*Department of Chemistry, Durham University, South Road, Durham DH1 3LE, United Kingdom*

(Received 19 December 2014; accepted 28 February 2015; published online 24 March 2015)

We report on the use of a liquid crystalline host medium to align single-walled carbon nanotubes in an electric field using an in-plane electrode configuration. Electron microscopy reveals that the nanotubes orient in the field with a resulting increase in the DC conductivity in the field direction. Current versus voltage measurements on the composite show a nonlinear behavior, which was modelled by using single-carrier space-charge injection. The possibility of manipulating the conductivity pathways in the same sample by applying the electrical field in different (in-plane) directions has also been demonstrated. Raman spectroscopy indicates that there is an interaction between the nanotubes and the host liquid crystal molecules that goes beyond that of simple physical mixing. © *2015 AIP Publishing LLC*. [http://dx.doi.org/10.1063/1.4916080]

I. INTRODUCTION

Carbon nanotubes possess unique electrical and mechanical properties and may be considered as one of the building blocks for nanotechnologies. This has led to significant scientific and technological activities in their exploitation. Examples of possible applications include chemical sensors,[1,2] carbon nanotube field-effect transistors,[3–5] active matrix organic light-emitting devices[6] and, most recently, evolvable computation.[7] For the latter application, external stimuli (e.g., electric fields) are applied to alter the behavior of a material system (evolution-in-materio). However, processing strategies are needed to enable the controlled assembly of the basic nano-components into larger, ordered architectures. A key requirement is a method to align the axes of both single- and multi-walled carbon nanotubes (SWCNTs and MWCNTs). One technique that has been attracting attention is the use of thermotropic liquid crystals (LCs) as solvents for the nanotubes.[8,9] This approach provides a simple means to control the alignment in both SWCNT and MWCNT thin films.

The first report of carbon nanotubes dispersed in liquid crystals was described by Lee and Chiu[10] in an attempt to exploit the composite in diffraction gratings. Subsequently, Lynch and Patrick[11] discussed the possibility of aligning the nanotubes with liquid crystal molecules. In 2004, Dierking and co-workers[12] achieved such an oriented structure and described electrical measurements based on the conductivity anisotropy of the nanotubes: a relatively high conductivity was found along the tube axes, but not across them. These studies have encouraged other workers to investigate this simple but versatile method to align nanotubes.[13–22] The majority of the work has used sandwich cells prepared from indium tin oxide (ITO) coated plates covered by a rubbed layer of polyimide as a basis for conducting the electrical and optical measurements. Here, we describe the use of simple coplanar electrodes to investigate the behavior of carbon nanotubes in a thin layer of a SWNCT/LC composite. This approach should allow the design of electrically conductive networks, the properties of which can be modified by externally applied fields.[7]

II. EXPERIMENTAL DETAILS

Mixed semiconducting and metallic SWCNTs were obtained from Carbon Nanotechnologies Inc. (Houston, TX, USA) in dried powder form. The unsorted material comprises about 2/3 of semiconducting and 1/3 of metallic nanotubes, with lengths varying from 100 nm to 1000 nm and diameters between 0.8 nm and 1.2 nm. The impurities represent less than 15% of the material according to the supplier. The nematic liquid crystal E7, a blend available from Merck Japan, is a mixture of four different liquid crystal molecules: 4-cyano-4′-n-pentyl-biphenyl (5CB), 4-cyano-4′-n-heptyl-biphenyl (7CB), 4-cyano-4′-n-oxyoctyl-biphenyl (8OCB) and 4-cyano-4″-n-pentyl-p-terphenyl (5CT). The materials were used as received.

The SWCNTs were dispersed in E7 by stirring for 24 h followed by 5 min of sonication, as reported by Schymura *et al.*[21] The final concentrations of the SWCNT/LC blends were 10^{-1} mg/ml, 10^{-3} mg/ml and 5×10^{-4} mg/ml (the units refer to milligrams of SWCNT per milliliters of liquid crystal); the equivalents in mass percentage are 1×10^{-2}%, 1×10^{-4}%, and 5×10^{-5}%. No additional surfactants or solvents were added to the solutions.

Gold electrodes were fabricated on 2 in. borosilicate glass wafers using etchback lithography. The metals were deposited by thermal evaporation; a chromium seed layer was used to aid gold adhesion to the glass. Figure 1(a) shows the completed wafer of electrodes; each electrode pair, Fig. 1(b), has an electrode gap of 50 μm × 1 mm. This area is shown in more detail in the optical micrograph to the right,

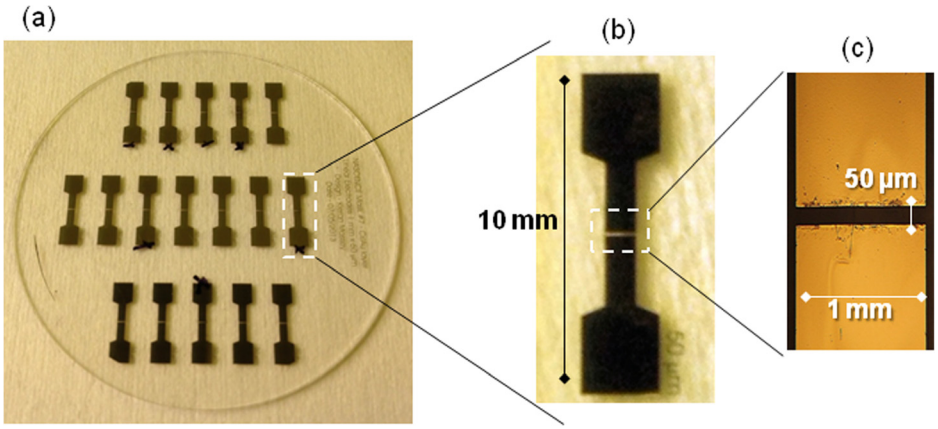

FIG. 1. (a) Photograph of the gold electrodes on a 2 in. glass wafer. (b) Photograph of an individual pair of electrodes. (c) Close-up micrograph of the electrode gap with a width of 1 mm and separation of 50 μm.

Fig. 1(c). A second design of electrode, produced by the same method, was used to explore alignment with crossed electrode pairs; this is introduced later in the paper (Figure 7). We used a micro-pipette tip to deposit the samples onto the electrodes gap. The needle tip was first soaked in the LC/SWCNT mixture; the electrode gap was then touched with this tip. Consequently, 1 to 5 μl of the material was transferred to the substrate.

Raman scattering spectra were recorded using a Horiba LabRam HR Evolution spectrometer equipped with a charge-coupled detector, in a backscatter geometry, using excitation wavelengths of 532 nm, 633 nm, and 785 nm. Spectra were recorded through a 1800 gr/mm grating, with a spot size of 1 μm through a $\times$50 long working distance objective. The spectral resolution is approximately 0.5 cm^{-1}. Five accumulations, each lasting 1 s, were taken over the range 100 cm^{-1} to 3000 cm^{-1}.

Fourier transform infrared (FTIR) spectra were recorded using a Perkin Elmer Spectrum 100 fitted with an attenuated total reflectance accessory. The spectral resolution was 4 cm^{-1}. Scanning electron microscope (SEM) images of the dried SWCNT/LC samples were recorded using a FEI Helios Nanolab 600 focused ion-beam electron microscope. The SEM micrographs were recorded at 5 kV, 7000$\times$ magnification in secondary electron or backscattered electron mode to study the nanotube distribution between the two electrodes.

A Vickers optical microscope with Canon EOS camera was used for the polarized image analysis. Two polarizers (one for incident and another one for transmitted light) were employed for monitoring images of the domains, one being fixed and the other used for the birefringence observations.

Current versus voltage (*I-V*) and current versus time (*I-t*) measurements were taken in air at room temperature with a Keithley 2635A sourcemeter, using an in-house MATLAB® measurement routine for the data acquisition.

III. RESULTS AND DISCUSSION

A. Microscopy

Optical polarizing microscopy and scanning electron microscopy were used to investigate the alignment of the SWCNTs in the composite films.[22] The optical images were acquired through polarizers placed at 90°; no subsequent software manipulation was used to enhance the images. Figure 2(a) shows a polarized optical microscope image collected from the area between the electrodes before the application of a voltage to a freshly-prepared sample, while Fig. 2(b) reveals the SEM image under identical conditions. The latter shows a random distribution of the SWCNT bundles, with no preferred direction of alignment. On the application of 7.5 V between the electrodes (1.5×10^5 V/m), both the optical and SEM images change. The former, Fig. 2(c), becomes much brighter and more homogeneous indicating orientation of the liquid crystal molecules in the applied field. This is consistent with the SEM image in Fig. 2(d) (acquired 2–3 days after the image in Fig. 2(c)), which clearly reveals changes in the distribution of the SWCNTs between the electrodes. A tendency of the nanotube bundles to drift towards one electrode was also evident in our experiments. This is probably related to the fact that the LC or

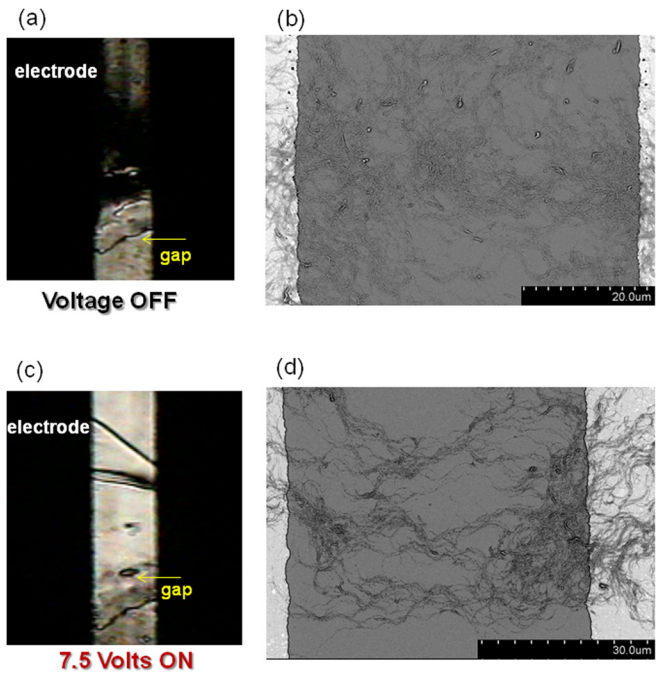

FIG. 2. Polarized optical microscope and SEM images. (a) A SWCNT/LC composite 10^{-1} mg/ml is placed on the electrode gap (50 μm) by drop casting; the optical image is acquired from the gap region before the voltage is applied. (b) SEM image from the sample under the same conditions. (c) Polarized optical image collected 30 s after the application of 7.5 V, and (d) SEM image collected after the application of the electric field.

SWCNT are charged species. Older LC displays, operated under DC voltages, exhibited polarization phenomena (leading to their AC operation).[23] Following removal of the electric field, the original (dark) optical image is observed suggesting that the LCs have relaxed to their previous random configuration. Video recordings showing the alignment process for both the pure LC (video 1-control experiment) and the 10^{-1} mg/ml composite (video 2) are provided as supplemental data.[24]

B. Electrical properties

Figure 3 shows *I-V* data for the three SWCNT/LC compositions (10^{-1} mg/ml, 10^{-3} mg/ml, and 5×10^{-4} mg/ml) over the voltage range 0 V to 12 V. The symbols represent three measurements, taken in sequence, from a freshly-prepared sample: circles represent the first sweep, triangles the second and squares the third. Each scan took about 5 s. Electrical measurements undertaken with the pure E7 (as a control) revealed negligible in-plane conductivity (data not shown). As a general observation, it is evident that all samples possess non-linear current versus voltage behavior. Furthermore, the electrical conductivity of each sample increases in the subsequent voltage scan, indicating a time-dependent effect. The greater the SWCNT concentration, the higher the conductivity of the composite is, suggesting that the electrical conduction pathway is through the network of carbon nanotubes. Although the average lengths of the individual semiconductive and metallic nanotubes ($\sim$1 μm) are significantly less than the electrode gap (50 μm), the SWCNTs will form bundles, or ropes, that are able to provide a percolation path between the electrodes.

We suggest that the time-dependent effects are associated with the movement of the carbon nanotubes in the SWCNT/LC composite film. In our work, the samples were subjected to electric fields up to 2.4×10^5 V/m (corresponding to 12 V), a similar value reported by Dierking *et al.*[12] for the alignment of carbon nanotubes dispersed in LC using traditional sandwich cells (electrode separations of about 6 μm). The movement of the liquid crystal may be imparted to the SWCNTs so that aligned nanotube bundles can be achieved.[12,25] In this case, the nanotubes follow the reorientation of LC director and demonstrate the guest-host effect known for molecular solutions and dispersions of anisotropic nanoparticles in LC hosts.[26,27] However, the lengths of the SWCNT bundles are significantly greater than the dimensions of individual LC molecules. An additional (perhaps dominant) effect, therefore, is that the nanotube bundles align directly in the applied electric field. The role of the liquid crystal host is simply to provide a low viscosity matrix, which facilitates the orientation of the nanotubes.

The time dependence of the electrical conductivity was further examined by measurements at a fixed applied voltage. Figure 4 shows three *I-t* curves for the different concentration mixtures with 7.5 V (1.5×10^6 V/m) applied for 30 min; the insets in each graph reveal expanded regions showing the current values on the first few seconds of the measurement. For all concentrations, an abrupt increase of the current is observed in the first few minutes; in the case of the lower

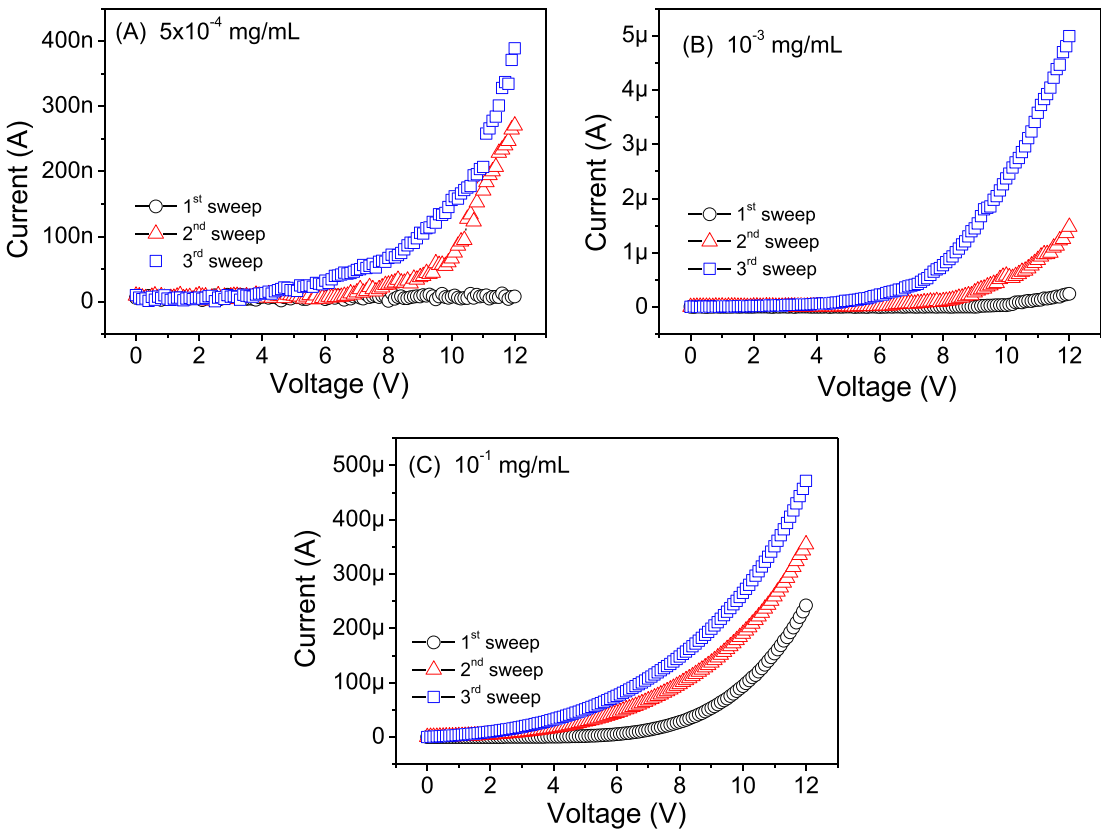

FIG. 3. Current-voltage characteristics (*I-V* curves) for three measurements taken in sequence using freshly prepared solutions with SWCNT concentration of (a) 5×10^{-4}, (b) 10^{-3} and (c) 10^{-1} mg/ml.

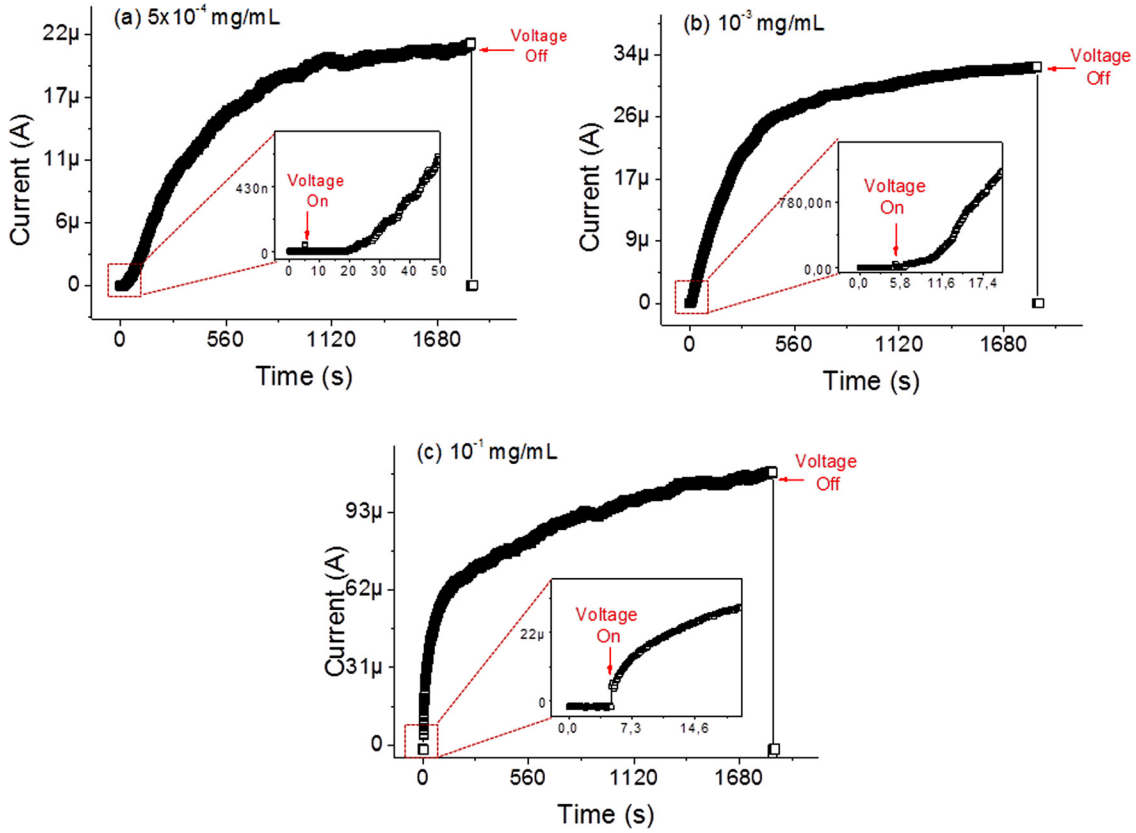

FIG. 4. Current-time measurements (*I-t* curves) for 7.5 V applied for 1800 s. The measurements were performed for solutions (a) 5×10^{-4}, (b) 10^{-3} and (c) 10^{-1} mg/ml.

SWCNT concentrations (5×10^{-4} and 10^{-3} mg/ml), a short delay is noted before the current begins to increase. This is followed by a more gradual increase in the current towards a saturation value. For the 5×10^{-4}, 10^{-3}, and 10^{-1} mg/ml concentrations, the maximum currents reached were approximately 23 μA, 32 μA, and 110 μA. This maximum current is approximately proportional to the cube root of the SWCNT concentration. Following removal of the applied voltage, the current immediately reverts to zero ("Voltage off" in the figure).

The timescale of the data presented in Fig. 4 should be contrasted to that of the experiments above (i.e., Fig. 3). In the latter case, by the end of the three sweeps, each of the samples had been subjected to the applied electric field for only about 15 s. This explains the significantly lower current values shown in Fig. 3 and provides further confirmation of the time dependence of the conductivity. This also suggests that longer exposure to an electrical field is most likely to lead to a greater number of conduction paths between the electrodes by virtue of the nanotubes aligning along the field direction.

Figure 5 shows the same conductivity data, but in a normalized format. Figure 5(a) compares the *I-t* curves for all concentrations subjected to a 1.5×10^5 V/m electric field. In contrast, Figure 5(b) reveals *I-t* curves for the 10^{-3} mg/ml solution exposed to different values of electric field. It is evident that both the nanotube concentration and voltage applied play important roles in the alignment process. We have attempted to fit the time-dependent conductivity data to a number of mathematical functions. The best fits were achieved using an exponential with two time constants, possibly associated with small and large bundles of nanotubes attempting to move under the influence of the applied electric field, i.e.,

$$y(x) = y_o + A_1(1 - e^{-\frac{x}{t_1}}) + A_2(1 - e^{-\frac{x}{t_2}}), \qquad (1)$$

where t_1 and t_2 are the two time constants, A_1 and A_2 are the amplitudes and y_0 represents an offset. The fits were chosen so that the R^2 factors (correlation coefficient) always exceeded 0.99. The time constant characterizing the initial fast rise of the signal (t_1) was found to depend on both the concentration of SWCNTs and the value of the electric field, as shown by the figures listed in Tables I and II. The initial amplitude A_1 also varied with both parameters, but not in a systematic way. The time constants controlling the slower part of the build-up (t_2), as well as their associated signal amplitudes A_2, were more difficult to determine reliably and their values exhibited somewhat irreproducible behavior. It is evident from Table I that the 10^{-1} mg/ml solution exhibits the fastest time constant for the first stage of alignment, while the 10^{-3} mg/ml composition is the one that reaches the highest maximum value. The data for different applied fields (Table II) show that an applied voltage of 10 V (2.0×10^5 V/m) produced the fastest and larger alignment for the first process, although the results are comparable to 7.5 V (1.5×10^5 V/m). These findings suggest that the time constants of the SWCNT/LC composite might be tailored for particular

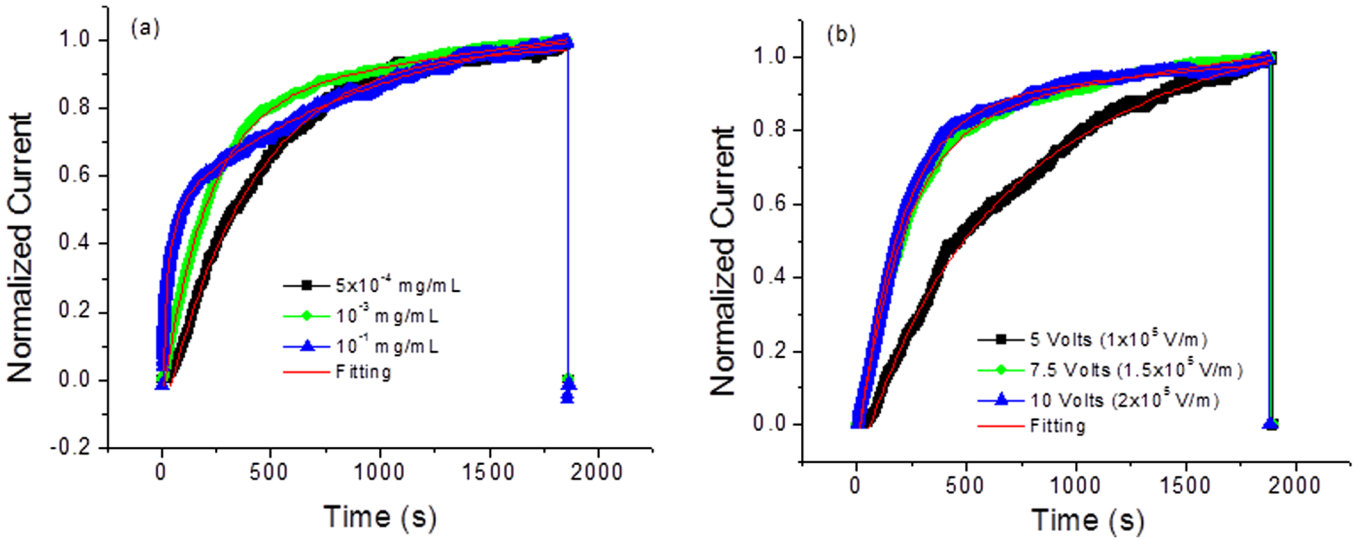

FIG. 5. (a) Normalized *I-t* curves for 7.5 V. (b) Normalized *I*−*t* curves for 5, 7.5, and 10 V applied to a thin film with a SWCNT concentration of 10^{-3} mg/ml.

applications, e.g., materials for memresistors[28] or evolutionary computation.[29]

The polarized microscopy experiments described earlier (see also supplemental data[24]) have suggested that the relatively small LC molecules can change their orientation when the electrical field is applied, but also when it is removed. One important question is does the induced alignment of the SWCNT molecules remain once the applied electric field has been removed? To address this, the samples were re-measured, and three *I-V* scans taken in rapid succession (5 s each, as before) following the *I-t* experiments (i.e., the samples had already been exposed for 30 min to an electric field of 10^5 V/m). The results are given in Figure 6. Figure 6(a) shows data for the 10^{-3} mg/ml thin film. The individual scans are very similar (unlike the data in Fig. 3), suggesting that the SWCNTs have been permanently aligned. The same study was repeated 45 days later following the storage of the samples in air with no field applied (the samples were still in their liquid form); the measured data (not shown) were very similar to those in Fig. 6(a), indicating that the nanotube alignment had been retained for, at least, six weeks.

Figure 6(b) shows *I-V* curves for each concentration following the *I-t* experiments described above. The plots are in the form of Log(*I*) versus Log(*V*). Two reasonably good straight lines (shown as full lines in Fig. 6(b)) can be fitted to each set of data; one for lower fields exhibiting a slope of 1.0 ± 0.1, and the second for higher fields with a slope of 2.0 ± 0.1. The lower conductivity regime can be accounted for by simple ohmic behavior. The break point between the high and low conductivity regimes is dependent on the SWCNT concentration, increasing in voltage with increasing nanotube concentration. This suggests that the conductivity process at high fields is dominated by space-charge effects, which generally exhibit a current versus voltage dependence of the form

$$I \propto V^n, \tag{2}$$

where n is an integer. In the case of single-carrier injection $n = 2$. The break point between the linear and quadratic regimes is determined by the intrinsic carrier concentration, n_0, in the thin film and for a simple single-carrier injection model, the voltage at which this occurs, V_x, is given by[30]

$$V_x = en_0 s^2/\theta\varepsilon_r\varepsilon_0, \tag{3}$$

where s is the distance between the electrodes, ε_r is the relative permittivity of the material and θ is the ratio of free to trapped charge. When the applied field is sufficiently high, the injected charge concentration becomes greater than the intrinsic charge density in the thin film, and superohmic conductivity is revealed. Clearly, the value of V_x does not scale with the nanotube concentration (Fig. 6). Other factors (θ, ε_r) must therefore be significant in determining the electrical behavior of our SWCNT/LC composite films.

We have also attempted to fit our data to other conductivity models, including Schottky emission and Poole-Frenkel conduction. The curves for one sample—corresponding to the 10^{-3} mg/ml concentration—were found to

TABLE I. Fast time constant and amplitude values extracted from the *I-t* curve fitting for different SWCNT concentrations (Fig. 5(a)).

SWCNT concentration (mg/ml)	t_1 (s)	A_1
5×10^{-4}	407	0.55
10^{-3}	209	0.89
10^{-1}	32	0.48

TABLE II. Fast time constant and amplitude values extracted from the *I-t* curve fittings for different electric fields applied to the 10^{-3} mg/ml solution (Fig. 5(b)).

Applied voltage (V) (electric field (V/m))	t_1 (s)	A_1
5 (10^5)	309	0.34
7.5 (1.5×10^5)	209	0.89
10 (2.0×10^5)	196	0.92

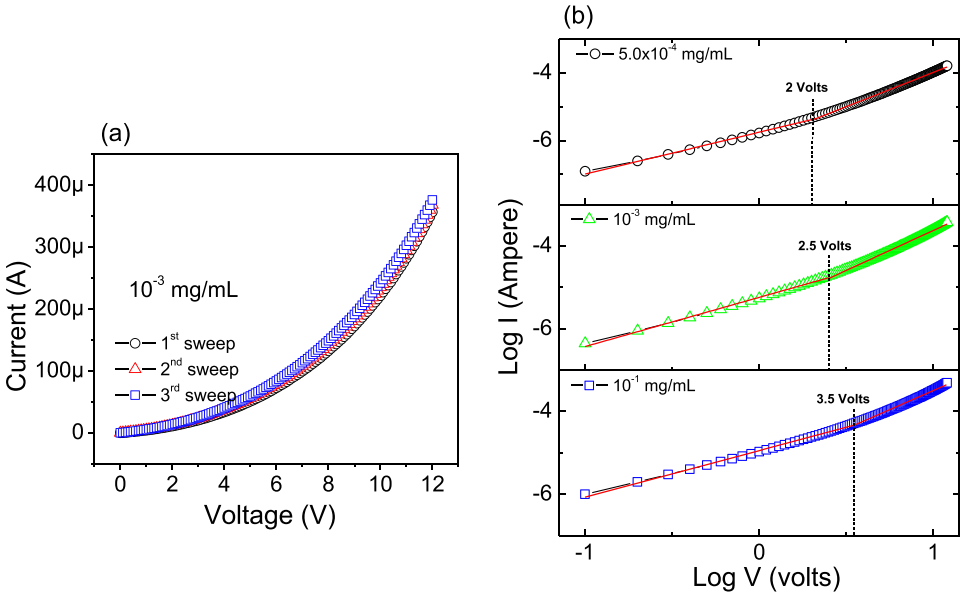

FIG. 6. Three *I-V* measurements taken in sequence following the *I-t* experiments using the 10^{-3} mg/ml SWCNT concentration sample. The samples were first polarized for 30 min with an electric field of 10^5 V/m, and then the *I-V* measurements measured in sequence. (b) Power law plot for *I-V* measurements (following *I-t* measurements) for the three concentrations investigated. Points represent experimental values. Full lines are best fits to a power law (see text for details).

exhibit an almost linear relationship between log $(\frac{I}{V})$ and $V^{\frac{1}{2}}$, characteristic of Poole-Frenkel conduction.[31] However, the figures obtained for the permittivity were unrealistic (with values much less than unity). The best fits over all our data sets were achieved using the above model of space-charge limited conduction.

We have also explored the effect of applying an electric field in a different alignment direction. The experimental arrangement and experimental results are depicted in Figure 7. Figure 7(a) shows the crossed planar electrode architecture developed to measure the current in two perpendicular directions, defined as direction X and direction Y. The inset shows

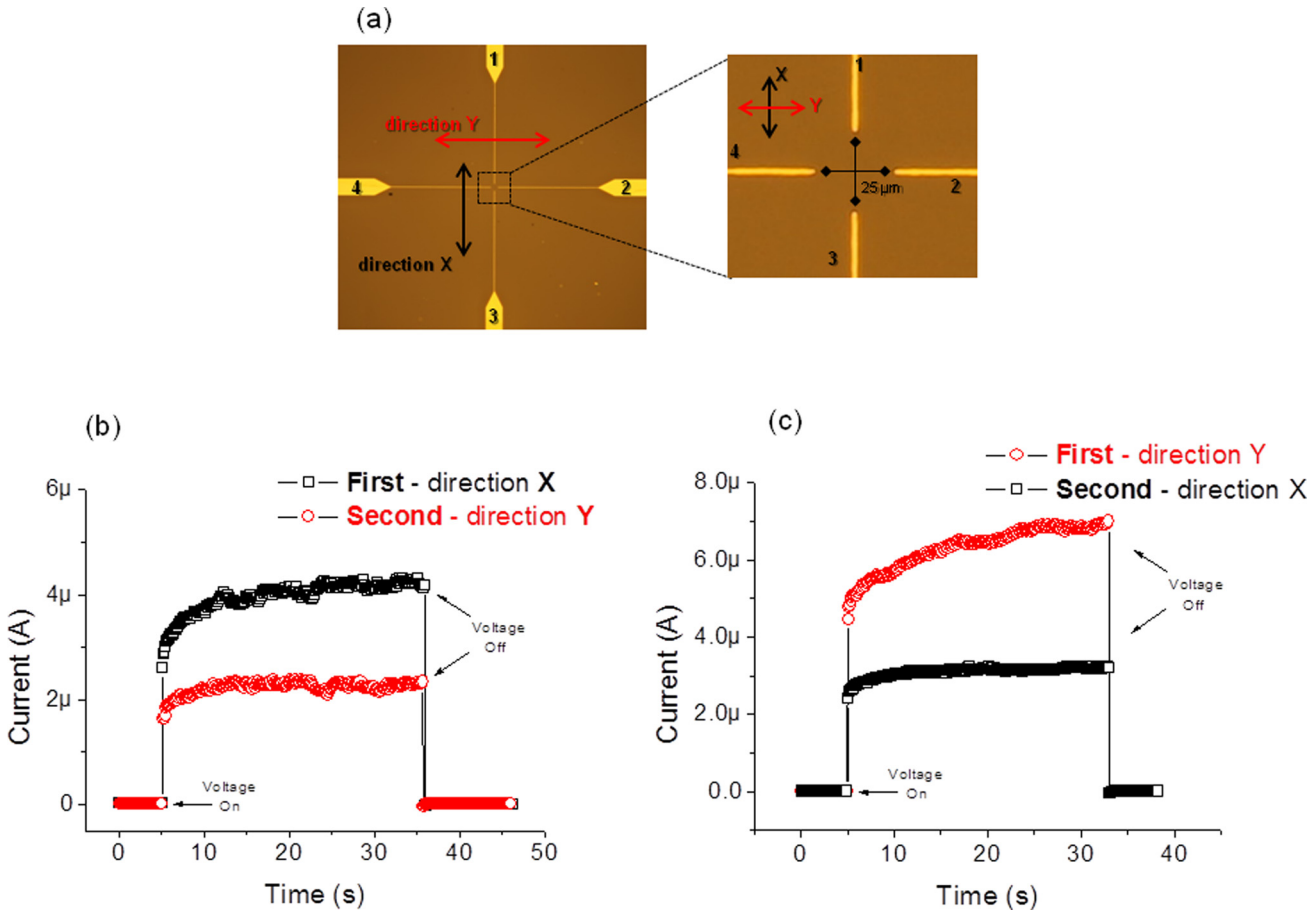

FIG. 7. (a) Four crossed electrodes utilized to investigate the conductivity in perpendicular directions, represented by direction X (between electrodes 1 and 3) and direction Y (electrodes 2 and 4). The gap between the electrodes is better seen in the inset: 25 μm with the electrode "fingers" 5 μm wide. (b) *I-t* curves for 10 V applied initially in direction X (square symbols), and then in direction Y (circle symbols). (c) The measurements repeated for the new sample, but now first in direction Y (circles) followed by direction X (squares).

the dimensional details for the electrode gap: 25 μm separation with an electrode track of 5 μm width. Current versus time data for 10 V (4.0×10^5 V/m) applied initially in direction X are shown by the square symbols in Fig. 7(b); the current reaches a value of about 4 μA after 30 s. The current was then monitored in direction Y with a voltage of 10 V applied in the same direction. In this case, the maximum current attained was ca. 2 μA. The shorter time for the currents to reach saturation in these experiments (i.e., compared to Fig. 4) is noteworthy. The most significant difference is the width of the electrodes: 5 μm in this measurement compared with 1 mm for the measurements shown in Fig. 4. We have previously suggested that the long time constant noted for the Fig. 4 data is related to large bundles of nanotubes attempting to move under the influence of the electric field. It is plausible that the much smaller electrodes used to obtain the data in Fig. 7 do not "support" these large bundles of nanotubes and that the time dependence of the conductivity simply reflects the faster movements of small bundles of SWCNTs.

As our electrode arrangement is symmetrical, the most likely explanation for the above direction-dependent data originates from the anisotropy in the conductivity of the SWCNTs. For the initial experiment, a significant number of the SWCNT bundles become aligned in the direction of the applied DC field and the conductivity is measured predominantly along the tube axes (direction X). Subsequent application of the field in an orthogonal direction results in a lower current, probably originating from two contributions: (i) the conductance of the originally aligned tubes across their lengths (radial conductance) and (ii) conductivity related to a few of the nanotube bundles that attempt to align in the new field direction.

To eliminate any interpretation due to possible inherent asymmetry in the electrode architecture, fresh samples were prepared. The electrical measurements were then conducted, first in direction Y and subsequently in direction X. The resulting data, Figure 7(c), confirm that the first measurement (either X or Y) always shows higher values of current. These results were reproducible over a period of several weeks and with experiments on more than ten samples. The conductivity measured in the first direction, be it X or Y, was always the higher.

C. Raman scattering and FTIR measurements

Fourier transform infrared and Raman spectroscopies were used to investigate the structural properties (chemical environment) of the LC/SWCNT composites, in an attempt to elucidate the possible interactions between the liquid crystal and SWCNT molecules. We have used the laser line at 633 nm to conduct the Raman scattering measurements since the vibrational characteristics of both molecules (E7 and SWCNT) reveal excellent definition at this excitation. Figure 8(a) shows Raman spectra collected for the three samples studied: pure E7, pure SWCNTs and the composite E7/SWCNT at a nanotube concentration of 10^{-1} mg/ml. Figure 8(b) shows the main bands in the low frequency range.

The spectrum of pure SWCNT differs considerably from other forms of carbon-based materials. The low-frequency bands in the region 100–300 cm^{-1} arise from the radial breathing modes (RBMs), which are the main characteristic of single- or few-walled carbon nanotubes (not present in graphite). The presence of multiple components at higher frequency, around 1500–1600 cm^{-1}, are associated with the lateral vibrational modes of the SWCNTs and are also a characteristic of this type of nanomaterial. In our sample, the individual components are the G^+ band, present at ca. 1580 cm^{-1}, and the G^- band at ca. 1544 cm^{-1}. These Raman features may be considered as spectral signatures of SWCNTs and have previously been used to characterize nanotube samples from their earliest stage of identification.[32–36] The other highlighted bands in the spectra are the D band and the G′ band, which are assigned to the disorder-

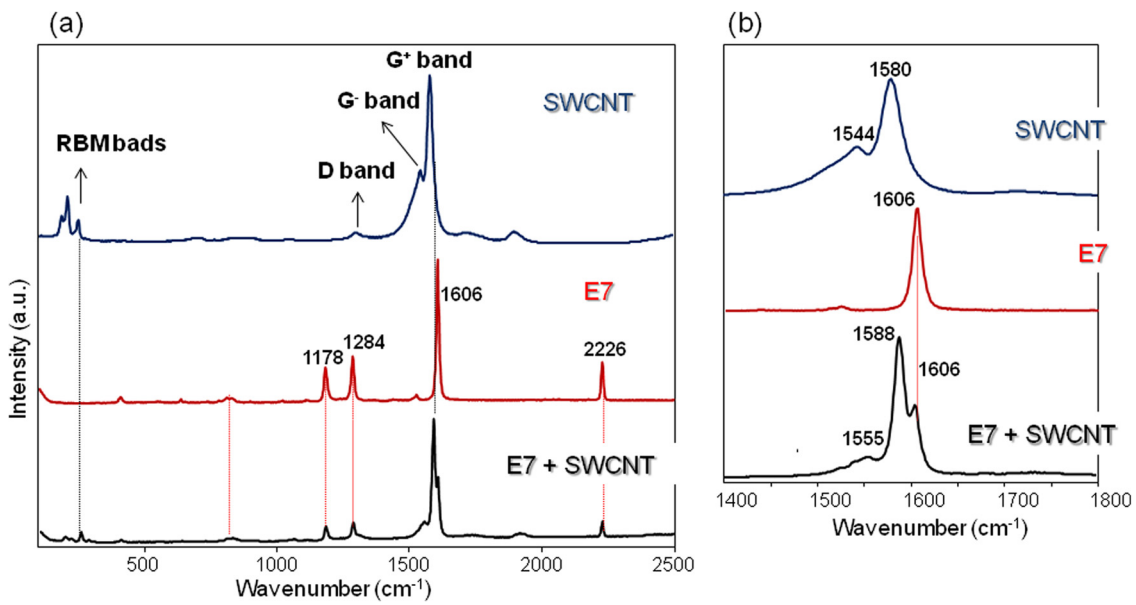

FIG. 8. (a) Raman scattering spectra using 633 laser line for pure liquid crystal E7, pure SWCNT and the composite E7 + SWCNT at 10^{-1} mg/ml. (b) The spectral region of the highest intensity peaks is enlarged to the left.

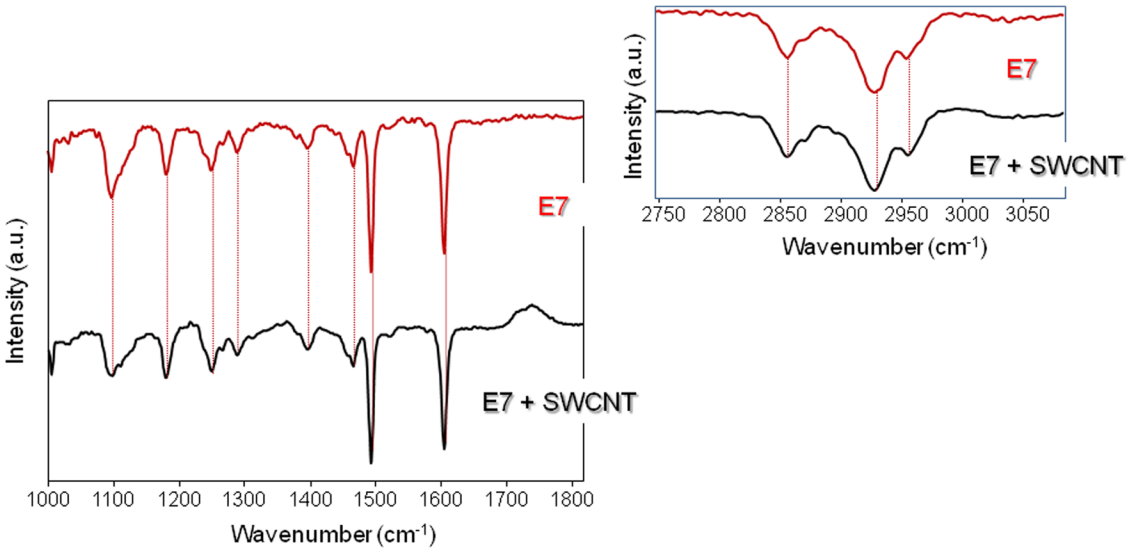

FIG. 9. FTIR spectra acquired for pure liquid crystal E7 and the composite E7 + SWCNT at 10^{-1} mg/ml.

induced in the nanotubes (D-band) between 1250 and 1450 cm^{-1} and its second-order band (G′ band) usually appearing between 2500 and 2900 cm^{-1} in Raman spectra of sp^2 carbon.[37] Although the D, G, and G′ modes are found in graphite, the RBM is specific to SWCNTs and may be exploited to determine their diameter and chirality.

The E7 liquid crystal is a multicomponent nematic mixture made by substituted 4-cyanobiphenyls (Sec. II).[38] The related Raman spectra collected using a 633 nm laser on a randomly aligned liquid crystal are also shown in Fig. 8, where the main vibrational modes are observed. The higher intensity Raman bands are assigned to the biphenyl ring deformations and the assignment of such modes has been performed by taking into account that biphenyl belongs to the C_{2v} point group.[39] The mode at 2226 cm^{-1} is assigned to CN stretching, while the mode at 1606 cm^{-1} is assigned to C=C stretching in the rings. The modes at 1178 and 1284 cm^{-1} are both assigned to C-H bending plus deformation of the biphenyl rings.[40]

By comparing the spectrum of the composite with those from the pure materials, we note a shift on the G^+ band from 1580 to 1588 cm^{-1} and in the G^- band from 1544 to 1555 cm^{-1} when the nanotubes are dispersed in E7. This, combined with changes in the RBMs, suggests molecular interaction between the SWCNTs and components of E7.[20] Conveniently, the band at 1606 cm^{-1} from E7, seen in the bulk and in the composites, can be used as an internal reference as it remains unchanged across the samples. The E7 1606 cm^{-1} band does not change as the majority of the liquid crystal remains in the bulk, remote from the SWCNT surface

Scalia *et al*. examined the interaction of SWCNTs and 5CB, a cyano bearing biphenyl and a component of E7.[20] The nature of the interaction was attributed to π-π stacking between the aromatic biphenyl and SWCNTs. Similarly Kimura *et al* also attributed π-π as the mechanism of interaction between carbon nanotubes and biphenyl cyano terminated oligo(phenylenevinylene).[41] Indeed, Beless *et al*. demonstrated that substituted biphenyl compounds, such as those in E7, are able to adsorb efficiently onto carbon nanotubes provided the aromatic rings were not sterically hindered against entering a plane with each other.[42]

The electron deficient cyano group, present on all the components of E7, are known to interact with SWCNTs[43,44] via the formation of a charge transfer complex. Harrison *et al*. reported cyano–SWCNT charge-transfer complexes to be the cause on upshifts in the SWCNT G band of +4 cm^{-1}.[45] This is consistent with earlier work, which demonstrated that electron withdrawal from SWCNTs results in an upshift in the G bands.[46,47] In contrast, π-π interactions in pyrene SWCNT systems generally report little or no change in the G band.[48]

It should be noted that the RBMs are more usually studied in π-π interactions. The RBMs of the SWCNT (633 nm excitation) were observed to upshift when in the presence of E7. However, upshifts have been reported for both π-π (Refs. 49 and 50) and charge-transfer interactions.[46] In addition, the RBMs are known to shift and change resonance in response to the degree of bundling.[49] Consequently, the RBMs do not provide any additional information other than there is an interaction between the E7 and SWCNTs. It is likely that the cyano groups are at least in part responsible for the strong interaction between the E7 and SWCNTs. Regardless of the mechanism, it is clear that there is an interaction between E7 and SWCNTs that goes beyond that of simple physical mixing. The fine chemical interaction between SWCNT and liquid crystal molecules might be, at least, important for the alignment process reported earlier.

FTIR absorption was also used to study the behavior of E7 in the composite film. Figure 9 contrasts the spectra for pure E7 and E7 + SWCNT collected in transmission mode. Apart from the small feature at around 1700 cm^{-1}, which is currently subject to further study, the FTIR data reveal no major changes in E7 when this material is present in the composite, corroborating the Raman results.

IV. CONCLUSION

We have reported on the alignment of single-walled carbon nanotubes in a matrix of a commercial liquid crystal

mixture. Optical and electron microscopies showed that the SWCNT ropes (or bundles) can be oriented by an in-plane electric field, although the precise role played by the LC molecules is unclear. Current versus voltage measurements on the composite revealed a nonlinear behavior, which was modelled using single-carrier space-charge injection. The possibility of manipulating the conductivity pathways in the same sample by applying the electrical field in different (in-plane) directions has also been demonstrated. The main Raman bands of the SWCNTs exhibited a shift to higher frequencies in the composite, indicating that the SWCNTs and E7 interact at the molecular level. Further experiments are ongoing to understand the precise role played by liquid crystalline molecules in the nanotube alignment process.

ACKNOWLEDGMENTS

The research leading to these results has received funding from the European Community's Seventh Framework Programme (FP7/2007-2013) under grant agreement number 317662 (NAnoSCale Engineering for Novel Computation using Evolution—NASCENCE, http://www.nascence.eu). One of the authors (DV) also thanks the São Paulo Research Foundation (FAPESP) for supporting this research (Grant No. 2013/08864-4). We also acknowledge the support from EU FP7 grants: *FUNPROB* (GA-269169), *NanoEmbrace* (GA-316751) and the Royal Academy of Engineering/Leverhulme Trust Senior Research Fellowship scheme.

[1]J. Kong, N. R. Franklin, C. W. Zhou, M. G. Chapline, S. Peng, K. J. Cho, and H. J. Dai, Science **287**, 622 (2000).
[2]A. Modi, N. Koratkar, E. Lass, B. Q. Wei, and P. M. Ajayan, Nature **424**, 171 (2003).
[3]I. Hwang, H. J. Jung, S. H. Cho, S. S. Jo, Y. S. Choi, J. H. Sung, J. H. Choi, M. H. Jo, and C. Park, Small **10**, 653 (2014).
[4]L. Zhang, X. Pan, and W. Wang, Nano **9**, 1450055 (2014).
[5]K. Keren, R. S. Berman, E. Buchstab, U. Sivan, and E. Braun, Science **302**, 1380 (2003).
[6]J. Zhang, Y. Fu, C. Wang, P.-C. Chen, Z. Liu, W. Wei, C. Wu, M. E. Thompson, and C. Zhou, Nano Lett. **11**, 4852 (2011).
[7]A. Kotsialos, M. K. Massey, F. Qaiser, D. A. Zeze, C. Pearson, and M. C. Petty, Int. J. Unconvent. Comput. **10**, 473–497 (2014).
[8]J. P. F. Lagerwall and G. Scalia, Curr. Appl. Phys. **12**, 1387 (2012).
[9]G. Scalia, ChemPhysChem **11**, 333 (2010).
[10]W. Lee and C. S. Chiu, Opt. Lett. **26**, 521 (2001).
[11]M. D. Lynch and D. L. Patrick, Nano Lett. **2**, 1197 (2002).
[12]I. Dierking, G. Scalia, P. Morales, and D. LeClere, Adv. Mater. **16**, 865 (2004).
[13]Y. Ji, Y. Y. Huang, and E. M. Terentjev, Langmuir **27**, 13254 (2011).
[14]B. R. Jian, C. Y. Tang, and W. Lee, Carbon **49**, 910 (2011).
[15]B. King and B. Panchapakesan, Nanotechnology **25**, 175201 (2014).
[16]S. Kumar and H. K. Bisoyi, Angew Chem. Int. Ed. **46**, 1501 (2007).
[17]L. N. Lisetski, S. S. Minenko, A. V. Zhukov, P. P. Shtifanyuk, and N. I. Lebovka, Mol. Cryst. Liq. Cryst. **510**, 43 (2009).
[18]M. Rahman and W. Lee, Key Eng. Mater. **428–429**, 173 (2010).
[19]G. Scalia, M. Haluska, U. Dettlaff-Weglikowska, F. Giesselmann, and S. Roth, AIP Conf. Proc. **786**, 114 (2005).
[20]G. Scalia, J. P. F. Lagerwall, M. Haluska, U. Dettlaff-Weglikowska, F. Giesselmann, and S. Roth, Phys. Status Solidi B **243**, 3238 (2006).
[21]S. Schymura, M. Kuhnast, V. Lutz, S. Jagiella, U. Dettlaff-Weglikowska, S. Roth, F. Giesselmann, C. Tschierske, G. Scalia, and J. Lagerwall, Adv. Funct. Mater. **20**, 3350 (2010).
[22]P. Van der Schoot, V. Popa-Nita, and S. Kralj, J. Phys. Chem. B **112**, 4512 (2008).
[23]L. Lu, A. Alagh, and P. J. Bos, Proc. SPIE **8114**, 811416-1 (2011).
[24]See supplementary material at http://dx.doi.org/10.1063/1.4916080 for video recordings of LC alignment.
[25]I. Dierking, K. Casson, and R. Hampson, Jpn. J. Appl. Phys. **47**, 6390 (2008).
[26]G. H. Heilmeie and L. A. Zanoni, Appl. Phys. Lett. **13**, 91 (1968).
[27]E. Sen, N. Kaya, and A. Alicilar, J. Mol. Liq. **186**, 33 (2013).
[28]A. Radoi, M. Dragoman, and D. Dragoman, Appl. Phys. Lett. **99**, 093102 (2011).
[29]S. L. Harding, J. F. Miller, and E. A. Rietman, Int. J. Unconvent. Comput. **4**, 155 (2008).
[30]C. F. Woellner and J. A. Freire, J. Chem. Phys. **134**, 084112 (2011).
[31]C. Cirtoaje, E. Petrescu, and C. Motoc, Physica E **54**, 242 (2013).
[32]R. Saito, A. Gruneis, G. G. Samsonidze, V. W. Brar, G. Dresselhaus, M. S. Dresselhaus, A. Jorio, L. G. Cancado, C. Fantini, M. A. Pimenta, and A. G. Souza, New J. Phys. **5**, 157 (2003).
[33]M. S. Dresselhaus, G. Dresselhaus, R. Saito, and A. Jorio, Phys. Rep. **409**, 47 (2005).
[34]M. S. Dresselhaus, G. Dresselhaus, and A. Jorio, J. Phys. Chem. C **111**, 17887 (2007).
[35]M. S. Dresselhaus, G. Dresselhaus, R. Saito, and A. Jorio, Cont. Concept Condens. **3**, 83 (2008).
[36]R. Saito, M. Hofmann, G. Dresselhaus, A. Jorio, and M. S. Dresselhaus, Adv. Phys. **60**, 413 (2011).
[37]M. S. Dresselhaus, G. Dresselhaus, A. Jorio, A. G. Souza, and R. Saito, Carbon **40**, 2043 (2002).
[38]A. R. E. Brás, T. Casimiro, J. Caldeira, and A. Aguiar-Ricardo, J. Chem. Eng. Data **50**, 1857 (2005).
[39]S.-W. Joo, T. D. Chung, W. C. Jang, M.-S. Gong, N. Geum, and K. Kim, Langmuir **18**, 8813 (2002).
[40]E. V. Astrova, T. S. Perova, S. A. Grudinkin, V. A. Tolmachev, Y. A. Pilyugina, V. B. Voronkov, and J. K. Vij, Semiconductors **39**, 759 (2005).
[41]M. Kimura, N. Miki, N. Adachi, Y. Tatewaki, K. Ohta, and H. Shirai, J. Mater. Chem. **19**, 1086 (2009).
[42]B. Beless, H. S. Rifai, and D. F. Rodrigues, Environ. Sci. Technol. **48**, 10372 (2014).
[43]D. Linton, P. Driva, B. Sumpter, I. Ivanov, D. Geohegan, C. Feigerle, and M. D. Dadmun, Soft Matter **6**, 2801 (2010).
[44]J. Lu, S. Nagase, X. W. Zhang, D. Wang, M. Ni, Y. Maeda, T. Wakahara, T. Nakahodo, T. Tsuchiya, T. Akasaka, Z. X. Gao, D. P. Yu, H. Q. Ye, W. N. Mei, and Y. S. Zhou, J. Am. Chem. Soc. **128**, 5114 (2006).
[45]K. E. Wise, C. Park, E. J. Siochi, and J. S. Harrison, Chem. Phys. Lett. **391**, 207 (2004).
[46]A. M. Rao, P. C. Eklund, S. Bandow, A. Thess, and R. E. Smalley, Nature **388**, 257 (1997).
[47]N. Bendiab, E. Anglaret, J. L. Bantignies, A. Zahab, J. L. Sauvajol, P. Petit, C. Mathis, and S. Lefrant, Phys. Rev. B **64**(24), 245424 (2001).
[48]Y. Zhang, S. L. Yuan, W. W. Zhou, J. J. Xu, and Y. Li, J. Nanosci. Nanotechnol. **7**, 2366 (2007).
[49]S. Debnath, Q. H. Cheng, T. G. Hedderman, and H. J. Byrne, Carbon **48**, 1489 (2010).
[50]S. Gotovac, H. Honda, Y. Hattori, K. Takahashi, H. Kanoh, and K. Kaneko, Nano Lett. **7**, 583 (2007).